PFC/JA-96-3-REV

MODE-CONVERSION OF FAST ALFVÉN WAVES AT THE ION-ION HYBRID RESONANCE

A. K. Ram, A. Bers, S. D. Schultz, and V. Fuchs

FEBRUARY 1996

Plasma Fusion Center
Massachusetts Institute of Technology
Cambridge, Massachusetts 02139 USA

This work was supported in part by DOE Grant No. DE-FG02-91ER-54109; by Atomic Energy of Canada Ltd, Hydro-Quebec, and Institut National de la Recherche Scientifique; and in part by TFTR (Tokamak Fusion Test Reactor) and TPX (Toroidal Physics Experiment).

To be published in *Physics of Plasmas (7th Annual Special Issue).*

MODE-CONVERSION OF FAST ALFVÉN WAVES AT THE ION-ION HYBRID RESONANCE

A. K. Ram, A. Bers, S. D. Schultz, and V. Fuchs

TABLE OF CONTENTS

Mode conversion of fast Alfvén waves at the ion-ion hybrid resonance

A. K. Ram,[1] A. Bers,[1] S. D. Schultz,[1] and V. Fuchs[2]

[1]Plasma Fusion Center, Massachusetts Institute of Technology, Cambridge, MA 02139

[2]Centre Canadien de Fusion Magnetique, Varennes, Québec, Canada

ABSTRACT

Substantial radio-frequency power in the ion-cyclotron range of frequencies can be effectively coupled to a tokamak plasma from poloidal current strap antennas at the plasma edge. If there exists an ion-ion hybrid resonance inside the plasma, then some of the power from the antenna, delivered into the plasma by fast Alfvén waves, can be mode converted to ion-Bernstein waves. In tokamak confinement fields the mode-converted ion-Bernstein waves can damp effectively and locally on electrons [A. K. Ram and A. Bers, Phys. Fluids B **3**, 1059 (1991)]. The usual mode-conversion analysis which studies the propagation of fast Alfvén waves in the immediate vicinity of the ion-ion hybrid resonance is extended to include the propagation and reflection of the fast Alfvén waves on the high magnetic-field side of the ion-ion hybrid resonance. It is shown that there exist plasma conditions for which the entire fast Alfvén wave power incident on the ion-ion hybrid resonance can be converted to ion-Bernstein waves. In this extended analysis of the mode conversion process, the fast Alfvén waves can be envisioned as being coupled to an internal plasma resonator. This resonator extends from the low magnetic-field cutoff near the ion-ion hybrid resonance to the high magnetic-field cutoff. The condition for 100% mode conversion corresponds to a critical coupling of the fast Alfvén waves to this internal resonator. As an example, the appropriate plasma conditions for 100% mode conversion are determined for the Tokamak Fusion Test Reactor (TFTR) [R. Majeski *et al., Proceedings of the 11th Topical Conference on RF Power in Plasmas*, Palm Springs (American Institute of Physics, N.Y., 1995), Vol. 355, p. 63] experimental parameters.

PACS: 52.25.Sw; 52.35.Hr; 52.55.Fa

I. INTRODUCTION

A most successful way of delivering radio frequency power for heating a tokamak plasma has been through fast Alfvén waves (FAW), excited by antennas on the low-field side of a tokamak, in the ion-cyclotron range of frequencies (ICRF). (The FAW is also sometimes referred to as the fast magnetosonic or fast compressional wave.) The coupling, propagation, and damping of FAW's have been extensively studied theoretically and demonstrated experimentally in a variety of tokamaks. In a plasma consisting of at least two ion species with different charge-to-mass ratios, the ion-ion hybrid resonance can be present in the plasma if the frequency of the RF wave is chosen appropriately. In the vicinity of this resonance, the FAW can couple to the ion-Bernstein wave (IBW), which then propagates away from the resonance towards the high-field side of the tokamak. Figure 1 shows the real part of $k_\perp^2$ for the FAW, obtained from the local hot (Maxwellian) plasma dispersion relation [1], when the ion-ion hybrid resonance is inside the plasma. ($k_\perp$ is the local value of the wave-vector perpendicular to the toroidal magnetic field and x is the distance along the equatorial plane of the tokamak; $x = 0$ being the center of the plasma.) The resonance behavior near $x = 0$ is indicative of the ion-ion hybrid resonance. A magnified view of the resonance region, given in Fig. 2, shows the coupling of the FAW to the IBW. Theoretical analysis has shown that these IBW's can damp effectively on electrons [2].

Recently, there has been a series of ICRF heating experiments in which the ion-ion hybrid resonance has been present inside the plasma (TFTR [3], Tore Supra [4], Alcator C-Mod [5]). The observed electron heating in these experiments has been attributed to the interaction of IBW's with electrons. In an earlier set of experiments on the Joint European Tokamak (JET) [6], it was observed that the lower-hybrid current drive (LHCD) efficiency increased in the presence of ICRF heating. The corresponding experimental conditions suggested that IBW's could be excited in the plasma. Theoretical analysis of the interaction of ICRF with LHCD showed that the interaction of IBW's with the LH-generated suprathermal electrons leads to an enhancement in the LHCD efficiency

[7]. In light of these experiments, it is useful to examine the mode-conversion process to IBW's with low-field side FAW excitation. For simplifying the analysis, we shall use a cold plasma model to represent the mode conversion by resonant absorption at the ion-ion hybrid resonance.

When the ion-ion hybrid resonance is inside a typical tokamak plasma, the FAW dispersion characteristics show that there are two right-hand cutoffs located in the outer regions of the plasma, on the high-magnetic field side and on the low-magnetic field side of the ion-ion hybrid resonance. In the vicinity of the resonance the FAW also has a left-hand cutoff. Previously, studies on the mode-conversion process have analyzed the propagation of the FAW in a region which includes the left-hand cutoff and the ion-ion hybrid resonance [8]. In this region, the propagation of the FAW can be described by the Budden equation [9,10]. The description is equivalent to the scattering of a wave by a potential having a resonance and a cutoff. The analysis shows that a maximum of 25% of the FAW power can be mode converted to IBW's. Recently, it has been noted that the high-field side right-hand cutoff can have a significant effect on the mode-conversion efficiency [11]. A physically motivated model analysis, and a more detailed phase-integral analysis of the problem which includes this cutoff have shown that, in contrast to the Budden problem, a maximum of 100% of the incident FAW power can be mode converted to IBW's [12]. In this paper, we derive an analytic solution of the mode conversion efficiency when the FAW is incident from the low-field side and encounters the left-hand cutoff, the ion-ion hybrid resonance, and the high-field side cutoff. We refer to this as the triplet case, which is equivalent to the Budden case with the addition of the right-hand cutoff. We derive an analytical expression for the mode-conversion coefficient, and show that the distance between the left-hand cutoff and the resonance is crucial in determining the maximum power that can be mode converted. The location of the right-hand cutoff is important in only determining if this maximum can be achieved in a given plasma configuration.

In Section II, we give a simple physical picture of the effect of the high-field side right-hand cutoff. We solve the Budden problem with the condition that the FAW is completely reflected at some point on the high-field side of the ion-ion hybrid resonance. In Section III,

we solve a model triplet problem with the high-field side right-hand cutoff. An approximate solution is obtained for the case when this right-hand cutoff is far from the ion-ion hybrid resonance (Sec. IIIa), and an exact solution is given for the case when the right-hand cutoff is close to the ion-ion hybrid resonance (Sec. IIIb). For both cases, we determine the mode-conversion and show the possibility of achieving 100% mode conversion efficiency. The results also show that the intuitive model of Section II is valid. In Section IV, we give a physical picture for understanding the analytical results.

II. BUDDEN PROBLEM WITH HIGH-FIELD SIDE REFLECTION

In a simple, one-dimensional (equatorial plane) description, the approximate cold-plasma dispersion relation for the FAW is:

$$n_\perp^2 = \frac{(L - n_\parallel^2)(R - n_\parallel^2)}{S - n_\parallel^2} \tag{1}$$

where $n_\perp = ck_\perp/\omega$, $n_\parallel = ck_\parallel/\omega$, ω is the frequency of the FAW, $k_\perp$ and $k_\parallel$ are the perpendicular (to the total magnetic field) and parallel wave vectors, respectively, and S, R, L are the usual Stix tensor elements that depend on the spatial coordinate [1]. In deriving Eq. (1) we assume that the FAW electric field component along the tokamak magnetic field is very small. $R = n_\parallel^2$ gives the positions of the right-hand cutoffs. There are usually two such cutoffs: one on the low magnetic field side near the antenna, and another on the high magnetic field side. The positions where $L = n_\parallel^2$ and $S = n_\parallel^2$ correspond to the left-hand cutoff and to the ion-ion hybrid resonance, respectively. The propagation of the FAW through the resonance and the cutoffs are described by a differential equation:

$$\frac{d^2E}{d\xi^2} + Q(\xi)E = 0 \tag{2}$$

where E is the poloidal component of the electric field, $\xi = \omega x/c$ is the normalized spatial coordinate along the equatorial plane, and $Q(\xi)$ is the "potential" function, which for a cold plasma is equal to the right-hand side of (1).

The usual Budden-type [9] mode-conversion analysis studies the asymptotic behavior of the solutions of (2) in the vicinity of the left-hand cutoff and the ion-ion hybrid resonance

(Appendix A). In this case, $Q(\xi)$ can be modelled by: $Q_B(\xi) = \gamma - \beta/\xi$ where $\sqrt{\gamma}$ is the normalized perpendicular wavenumber (which is the perpendicular wave index $n_\perp$) of the FAW and β/γ defines the normalized distance (normalized to c/ω) between the left-hand cutoff and the ion-ion hybrid resonance (at $\xi = 0$). For a FAW incident from the low-field side ($\xi > 0$), the Budden-type analysis gives the transmission through the left-hand cutoff and resonance, and the reflection from the left-hand cutoff. From power conservation, the difference between the incident FAW power and the sum of the transmitted and reflected FAW power gives the power that is mode converted. An analysis of the Budden problem shows that the maximum fraction of the incident FAW power that can be mode converted is 25% (Appendix A).

In order to intuitively understand the effect of the high-field side right-hand cutoff, let us assume that, for a wave incident from the low field side ($\xi > 0$), there is a reflection boundary at some point $\xi = \xi_R$ ($\xi_R < 0$). Then the FAW transmitted through the resonance gets reflected back towards the resonance from the high-field side. In this case, the transmission beyond the cutoff is zero, since waves do not propagate for $\xi < \xi_R$. There is only a power reflection coefficient and a power mode-conversion coefficient. The general solution, in terms of the Whittaker functions [13], is given by:

$$E(\xi) \;=\; c_1 W_{\kappa,1/2}(z) \;+\; c_2 W_{-\kappa,1/2}(-z) \tag{3}$$

where c_1 and c_2 are arbitrary constants that depend on the boundary conditions, and

$$z \;=\; -2i\sqrt{\gamma}\xi,\; \kappa \;=\; -\frac{i}{2}\frac{\beta}{\sqrt{\gamma}} \;\equiv\; -\frac{i}{2}\eta\;. \tag{4}$$

For $\xi \to -\infty$, $W_{\kappa,1/2}(z)$ represents an incoming (towards $\xi = 0$) wave while $W_{-\kappa,1/2}(-z)$ represents an outgoing wave. For $\xi \to \infty$ $W_{\kappa,1/2}(z)$ represents an outgoing wave while $W_{-\kappa,1/2}(-z)$ is a combination of an incoming wave and an outgoing wave (Appendix A). If we assume that there is no damping of the wave between the resonance and the high-field cutoff, then c_1 and c_2 differ by at most an arbitrary phase. Let us assume that $c_2 = c_1 \exp[-i(\pi + \phi)]$. Then, using the asymptotic properties of the Whittaker functions

for $\xi \to \infty$ (Appendix A), the power reflection coefficient is:

$$R = e^{-2\pi\eta}\left|1 + e^{-i\phi}\frac{2\pi i e^{\pi\eta/2}}{\Gamma(-i\eta/2)\Gamma(1-i\eta/2)}\right|^2 \tag{5}$$

Using the properties of the Gamma function [13] it can be shown that:

$$\begin{aligned} R(\eta,\phi) &= (1-T_B)^2 + T_B^2 - 2T_B(1-T_B)\cos(\phi+2\theta) \\ &= 1 - 4T_B(1-T_B)\cos^2\left(\frac{\phi}{2}+\theta\right) \end{aligned} \tag{6}$$

where $T_B = \exp(-\pi\eta)$ and θ is the phase of $\Gamma(-i\eta/2)$. Then the power-mode conversion coefficient $C = 1 - R$ is:

$$C(\eta,\phi) = 4T_B(1-T_B)\cos^2\left(\frac{\phi}{2}+\theta\right) \tag{7}$$

Hence, with a high-field side cutoff the maximum power mode-conversion coefficient can be 100% provided $T_B = 1/2$ and $(\phi/2 + \theta)$ is an integer multiple of π. Thus, the effect of a high-field side reflection in the Budden problem can significantly alter the power mode converted. In Fig. 3, we have plotted contours of constant $C(\eta,\phi)$ as functions of ϕ and η. These contours are periodic in ϕ modulo 2π. From this figure, it is clear that the maximum value of C is critically dependent on η — the product of the distance between the left-hand cutoff and the ion-ion hybrid resonance, with the perpendicular wavenumber of the incident FAW. For example, for $\eta > 0.3$ it is not possible to get 100% mode conversion regardless of the choice of the phase ϕ.

In Fig. 4, we plot the curves of maximum mode-conversion coefficient as a function of the peak electron density and of $k_\parallel$ for TFTR parameters. From (7) the maximum mode-conversion coefficient is a function of η only. So this figure shows the dependence of η on density and $k_\parallel$.

III. SOLUTION OF THE TRIPLET PROBLEM

We now address solving the complete triplet problem without introducing an unspecified reflection phase at the high-field right-hand cutoff. For this, we find it convenient to

consider two models for the overall potential: one for which the right-hand cutoff is far from the resonance, and thus separated from it by a region in which WKB solutions are appropriate; and the other for which the right-hand cutoff can be near the resonance.

A. High-Field Cutoff Far From Resonance

For the propagation of FAW in a one-dimensional slab where the high-field cutoff is included in the description of the model, the model potential in (2) is given by:

$$Q(\xi) = \begin{cases} \gamma - \dfrac{\beta}{\xi}, & \text{if } \xi > 0 \\ \alpha\xi + \tilde{\gamma} - \dfrac{\beta}{\xi}, & \text{if } \xi \leq 0 \end{cases} \tag{8}$$

and α, β, γ, and $\tilde{\gamma}$ are parameters that are determined from a fit to the local fast wave dispersion relation. For $\xi > 0$ (8) gives the usual Budden potential with $\gamma > 0$ and $\beta > 0$. The right-hand cutoff is given by $Q(\xi) = 0$ for $\xi < 0$. We will assume that near the right-hand cutoff $|\beta/\xi|$ is very small compared to $|\alpha\xi|$ and $\tilde{\gamma}$, so that this cutoff is approximately given by $\xi_R = -\tilde{\gamma}/\alpha$. Since for $\xi < \xi_R$ we assume that the solutions to (1) are evanescent, it follows that $\alpha > 0$ and $\tilde{\gamma} > 0$. A model $Q(\xi)$ plotted in Fig. 5 shows characteristics very similar to those of the FAW dispersion relation between the high-field side cutoff and the left-hand cutoff.

The solution to (2) is obtained by determining the solutions for $\xi < 0$ (referred to as region I) and for $\xi > 0$ (region II) and matching them across $\xi = 0$. In region II, the solutions are given by the usual Whittaker functions discussed earlier. In region I, there does not exist a closed form solution in terms of known functions. However, by subdividing region I into three sub-regions and doing asymptotic matching across these three sub-regions, we obtain an approximate solution in region I (Appendix B). The matching conditions at $\xi = 0$ are:

$$\begin{aligned} E_{II}(\xi)\Big|_{\xi\to 0+} &= E_I(\xi)\Big|_{\xi\to 0-} \\ \frac{dE_{II}(\xi)}{d\xi}\Big|_{\xi\to 0+} &= \frac{dE_I(\xi)}{d\xi}\Big|_{\xi\to 0-} + i\pi\beta E(0) \end{aligned} \tag{9}$$

where 0^+ or 0^- indicates that ξ tends to zero from the positive or the negative side, respectively. The jump condition for the derivative of E can be easily derived since near

$\xi = 0$ the potential function is of the form $-\beta/\xi$. This gives the logarithmic singularity in ξ. Using the convention discussed in Appendix A, we define $\ln(0^+/0^-) = i\pi$.

The high-field cutoff ξ_R ensures that the power transmission coefficient is zero. The solution to (2) and (8) will determine the power reflection coefficient R. The mode-conversion coefficient will be $C = 1 - R$. The solution in region II can be written as:

$$E_{II}(x) = c_{II} W_{\kappa,1/2}(z) + d_{II} W_{-\kappa,1/2}(-z) \tag{10}$$

where c_{II} and d_{II} are constants determined by the boundary conditions, and z and κ are as defined for the Budden problem discussed in the previous section. From the asymptotic forms of the Whittaker functions (Appendix A), the power reflection coefficient can be expressed as:

$$R = \left| \frac{c_{II}}{d_{II}} - (1 - \mathrm{e}^{\pi\eta})\,\mathrm{e}^{-2i\theta} \right|^2 \mathrm{e}^{-2\pi\eta} \tag{11}$$

where θ is the phase of $\Gamma(-i\eta/2)$. The ratio c_{II}/d_{II} is determined by matching to the solution in region I. In region I, as $\xi \longrightarrow 0^-$, the solution to (2) and (8) is:

$$\lim_{\xi \to 0^-} E_I(\xi) = c_I W_{\tilde{\kappa},1/2}(\tilde{z}) + d_I W_{-\tilde{\kappa},1/2}(-\tilde{z}) \tag{12}$$

where c_I and d_I are constants, and

$$\tilde{z} = -2i\sqrt{\tilde{\gamma}}\xi, \quad \tilde{\kappa} = -\frac{i}{2}\frac{\beta}{\sqrt{\tilde{\gamma}}} \equiv -\frac{i}{2}\tilde{\eta}\,. \tag{13}$$

From the matching conditions in (9) at $\xi = 0$, and using the properties of the Whittaker functions near $\xi = 0$ [14], we find:

$$\frac{c_{II}}{d_{II}} = e^{-2i\theta}\, \frac{\frac{c_I}{d_I} e^{2i\tilde{\theta}} \left\{ A + i\pi + i\pi \coth\left(\frac{\pi\eta}{2}\right) \right\} - \left\{ A + i\pi \coth\left(\frac{\pi\eta}{2}\right) - i\pi \coth\left(\frac{\pi\tilde{\eta}}{2}\right) \right\}}{\frac{c_I}{d_I} e^{2i\tilde{\theta}} A - \left\{ A - i\pi - i\pi \coth\left(\frac{\pi\tilde{\eta}}{2}\right) \right\}} \tag{14}$$

where

$$A = \frac{1}{2}\ln\left(\frac{\tilde{\gamma}}{\gamma}\right) + \psi_R\left(\frac{i\tilde{\eta}}{2}\right) - \psi_R\left(\frac{i\eta}{2}\right) + i\frac{\pi}{2}\left\{ \coth\left(\frac{\pi\tilde{\eta}}{2}\right) - \coth\left(\frac{\pi\eta}{2}\right) \right\} \tag{15}$$

$\tilde{\theta}$ is the phase of $\Gamma(-i\tilde{\eta}/2)$, and ψ_R is the real part of the Psi function [13].

An approximate solution in region I is obtained by uniform asymptotic matching (Appendix B). We find:

$$\frac{c_I}{d_I} = -i\left(\frac{\alpha}{8i\tilde{\gamma}^{3/2}}\right)^{-i\tilde{\eta}} \exp\left(\frac{\pi\eta}{2}\right) \exp\left(\frac{4i}{3\alpha}\tilde{\gamma}^{3/2}\right) . \tag{16}$$

Since from (16) $|c_I/d_I| = 1$, it can be shown that, from (14), $|c_{II}/d_{II}| = 1$. Thus, we can express $c_{II}/d_{II} = \exp[i(\pi + \phi)]$ where the expression for ϕ can be determined from (14) and (16). Substituting this into (11) completely determines the reflection coefficient.

In the special case when $\tilde{\gamma} = \gamma$, we find from (14) and (16) that the phase ϕ is given by:

$$\begin{aligned} \phi &= \frac{4}{3\alpha}\gamma^{3/2} + \eta \ln\left(\frac{8\gamma^{3/2}}{\alpha}\right) + \frac{\pi}{2} \\ &= \frac{4\sqrt{\gamma}}{3|\xi_R|} + \eta \ln\left(\frac{8\sqrt{\gamma}}{|\xi_R|}\right) + \frac{\pi}{2} \end{aligned} \tag{17}$$

where $\xi_R < 0$ is the location of the right-hand cutoff. Thus, the phase introduced by the right-hand cutoff is related to the distance between the resonance and the right-hand cutoff normalized to the FAW wavelength.

B. High-Field Cutoff Close to Resonance

In the case when the high-field cutoff is close to the resonance, the potential can be approximated by:

$$Q(\xi) = \begin{cases} \gamma - \dfrac{\beta}{\xi}, & \text{if } \xi > 0 \\ -\overline{\gamma} - \dfrac{\beta}{\xi}, & \text{if } \xi \leq 0 \end{cases} \tag{18}$$

where β, γ, and $\overline{\gamma}$ are all positive parameters. Here the right-hand cutoff is at $\xi = -\beta/\overline{\gamma}$. The solution to (2) and (18) is given by the Whittaker function in the two regions ($\xi > 0$ and $\xi \leq 0$). The matching of the solutions across $\xi = 0$, in a manner similar to that described above, gives the mode-conversion coefficient in the form of (7). The phase ϕ is given exactly by:

$$\phi = \pi + \cos^{-1}\left(\frac{N_R^2 - N_I^2}{N_R^2 + N_I^2}\right) - 2\theta \tag{19}$$

where N_R and N_I are the real and imaginary parts of N, respectively, and

$$N = \ln\left(\frac{i\eta}{\overline{\eta}}\right) + \pi\left\{i\coth\left(\frac{\pi}{2}\eta\right) + \cot\left(\frac{\pi}{2}\overline{\eta}\right)\right\} - \frac{1}{\overline{\eta}} - \frac{i}{\eta} + \psi\left(1 + \frac{1}{2}\overline{\eta}\right) - \psi\left(1 + \frac{i}{2}\eta\right) \quad (20)$$

ψ is the Psi function [13], and $\overline{\eta} = \beta/\sqrt{\overline{\gamma}}$. We note that the overall result for the mode-conversion coefficient (7) is again the same as found in Sec. II. The phase (19) is now exactly determined; it can no longer be easily interpreted in terms of the distance between the resonance and the right-hand cutoff.

IV. THE INTRINSIC INTERNAL RESONATOR

The analyses of sections II and III imply that the triplet system can be viewed as forming an internal plasma resonator which contains resonant absorption. The resonator is intrinsic to the plasma in that it does not require a structure external to the plasma — it is formed by features (the cutoffs) that are intrinsic to the plasma. The fast Alfvén wave incident from the low-field side is coupled to the resonator at the left-hand cutoff. This coupling is mainly determined by η which enters into $T_B = \exp(-\pi\eta)$. The resonator is naturally specified by the phases ϕ and θ. However, due to the intrinsically inhomogeneous plasma, these phases are not simply related to some integer multiple of half-wavelengths between the left-hand cutoff and high-field side right-hand cutoff. The dissipation in this resonator occurs at the ion-ion hybrid resonance layer. In the cold plasma model, this is exhibited as resonant absorption; a kinetic description of the ion-ion hybrid resonance layer shows that this is mode conversion of the incident fast Alfvén wave to an ion-Bernstein wave which damps on electrons [2]. The condition for 100% mode conversion corresponds to the situation in which the incident fast Alfvén wave is critically coupled to this resonator. Then there is no reflection of the fast Alfvén wave towards the low-field side, and the incident wave power is totally absorbed. Figure 6 shows an example of the internal resonator effect where we have chosen parameters such that $\eta \approx 0.22$. Here there is no reflection and the fields are localized between the resonance and the high-field cutoff.

V. CONCLUSIONS

Through a detailed analysis of the effect of the high-field side right-hand cutoff on the mode conversion of the fast Alfvén wave at the ion-ion hybrid resonance, we have shown that there exist conditions for achieving 100% mode conversion to ion-Bernstein waves. The important parameter in achieving high mode conversion efficiencies is η, which is essentially the distance between the left-hand cutoff and the ion-ion hybrid resonance normalized to the wavelength of the fast Alfvén wave. For $\eta = \log(2)/\pi \approx 0.2206$, the phase of $\Gamma(-i\eta/2)$ is $\theta \approx 0.52\pi$. Then, if the high-field side right-hand cutoff is not too close to the ion-ion hybrid resonance, from (7) for $\phi \approx 2(l - 0.52)\pi$, where l is any integer, the mode conversion efficiency is 100%. This is the condition for critical coupling to an internal plasma resonator composed of the left-hand cutoff, the ion-ion hybrid resonance, and the high-field side right-hand cutoff.

ACKNOWLEDGEMENTS

This work is supported by Department of Energy Grant No. DE-FG02-91ER-54109, by Atomic Energy of Canada Ltd, Hydro-Quebec, and Institut National de la Recherche Scientifique, and in part by TFTR (Tokamak Fusion Test Reactor) and TPX (Toroidal Physics Experiment).

APPENDIX A: SOLUTION TO THE BUDDEN EQUATION

As in [9], the second order differential equation:

$$\frac{d^2E}{d\xi^2} + \left(\gamma - \frac{\beta}{\xi}\right) E = 0 \qquad (A1)$$

can be expressed in the standard Whittaker form [13]:

$$\frac{d^2E}{dz^2} + \left(-\frac{1}{4} - \frac{\frac{i\eta}{2}}{z}\right) E = 0 \qquad (A2)$$

where $z = -2i\sqrt{\gamma}\xi$ and $\eta = \beta/\sqrt{\gamma}$. The two independent solutions are given by the Whittaker functions $W_{\kappa,\mu}(z)$ and $W_{-\kappa,\mu}(-z)$ where $\kappa = -i\eta/2$ and $\mu = \pm 1/2$. In order to determine the scattering coefficients for (A1), we need to know only the asymptotic forms of the Whittaker functions.

In (A1), there is a pole at $\xi = 0$. Since we assume a time dependence of the form $\exp(-i\omega t)$, there is a branch cut in the upper-half complex-ξ plane starting at $\xi = 0$ (see [9] for a detailed argument). Thus, for $\xi < 0$ we define $\xi = |\xi|\exp(-i\pi)$. With this convention, the asymptotic forms of the Whittaker functions are given by [15]:

<u>for $\xi \to \infty$</u>

$$\begin{aligned}
W_{\kappa,1/2}(z) &\sim z^{\kappa} e^{-z/2} \\
&= |2\sqrt{\gamma}\xi|^{-i\eta/2} e^{-\pi\eta/4} e^{i\sqrt{\gamma}\xi} \\
W_{-\kappa,1/2}(-z) &\sim \left(z^{-\kappa} e^{z/2} - \frac{2\pi i}{\Gamma\left(\frac{1}{2} - \mu + \kappa\right)\Gamma\left(\frac{1}{2} + \mu + \kappa\right)} z^{\kappa} e^{-z/2} \right) e^{i\pi\kappa} \\
&= |2\sqrt{\gamma}\xi|^{i\eta/2} e^{3\pi\eta/4} e^{-i\sqrt{\gamma}\xi} - \frac{2\pi i}{\Gamma\left(\frac{-i\eta}{2}\right)\Gamma\left(1 - \frac{i\eta}{2}\right)} |2\sqrt{\gamma}\xi|^{-i\eta/2} e^{\pi\eta/4} e^{i\sqrt{\gamma}\xi}
\end{aligned} \qquad (A3)$$

for $\xi \to -\infty$

$$\begin{aligned} W_{\kappa,1/2}(z) &\sim z^{\kappa} e^{-z/2} \\ &= |2\sqrt{\gamma}\xi|^{-i\eta/2} e^{\pi\eta/4} e^{i\sqrt{\gamma}\xi} \\ W_{-\kappa,1/2}(-z) &\sim z^{-\kappa} e^{i\pi\kappa} e^{z/2} \\ &= |2\sqrt{\gamma}\xi|^{i\eta/2} e^{\pi\eta/4} e^{-i\sqrt{\gamma}\xi} \end{aligned} \tag{A4}$$

where Γ is the Gamma function [13].

In the usual Budden problem for low-field incidence, the relevant solution to (A1) is $W_{-\kappa,1/2}(-z)$. Then, it can be easily shown that the Budden power transmission and power reflection coefficients are:

$$\begin{aligned} T_B &= e^{-\pi\eta} \\ R_B &= (1 - T_B)^2 \end{aligned} \tag{A5}$$

respectively. The power mode-conversion coefficient is:

$$C_B = 1 - T_B - R_B = T_B(1 - T_B) \tag{A6}$$

which attains a maximum value of $1/4$ for $T_B = 1/2$.

APPENDIX B: SOLUTION TO THE TRIPLET EQUATION

We will use the method of matched asymptotic expansions [16] to construct an approximate solution to the differential equation in region I. With this solution we can determine the ratio c_{II}/d_{II} needed to calculate the reflection coefficient in (11). Region I is subdivided into three regions: region IA, corresponding to $\xi \lesssim \xi_R$; region IB, corresponding to $\xi > \xi_R$ and $\xi < 0$; and region IC, corresponding to $\xi \approx 0$. By approximating $Q(\xi)$ in each of these sub-regions, we can determine the corresponding approximate solutions. By matching these approximate solutions across the boundaries of the corresponding sub-regions, we determine the solution in region I.

In region IA, $Q(\xi) \approx \alpha\xi + \tilde{\gamma}$ so that $\xi_R \approx -\tilde{\gamma}/\alpha$. The solution to $E(\xi)$ is of the form:

$$E_{IA}(\xi) = c_1 \mathrm{Ai}\left(-\alpha^{1/3}\left\{\xi + \frac{\tilde{\gamma}}{\alpha}\right\}\right) + d_1 \mathrm{Bi}\left(-\alpha^{1/3}\left\{\xi + \frac{\tilde{\gamma}}{\alpha}\right\}\right) \tag{B1}$$

where Ai and Bi are the Airy functions [13] and c_1 and d_1 are constants. For $\xi \to -\infty$ we require a decaying solution, so that from the asymptotics of the Airy functions, $d_1 = 0$.

In region IC we approximate $Q(\xi) \approx \widetilde{\gamma} - \beta/\xi$. The solution to $E(\xi)$ is in terms of the Whittaker functions:

$$E_{IC}(\xi) \;=\; c_3 W_{\widetilde{\kappa},1/2}(\widetilde{z}) + d_3 W_{-\widetilde{\kappa},1/2}(-\widetilde{z}) \qquad (B2)$$

where c_3 and d_3 are constants, and the rest of the notation is as defined in (13).

In region IB, which is assumed to be sufficiently far away from the right-hand cutoff and from the resonance, we assume a solution of the JWKB form:

$$E_{IB}(\xi) \;=\; \frac{c_2}{[Q(\xi)]^{1/4}} \mathrm{e}^{\,i\int_{\xi_R}^{\xi} d\xi' \sqrt{Q(\xi')}} + \frac{d_2}{[Q(\xi)]^{1/4}} \mathrm{e}^{\,-i\int_{\xi_R}^{\xi} d\xi' \sqrt{Q(\xi')}} \qquad (B3)$$

where $Q(\xi) = \alpha\xi + \widetilde{\gamma} - \beta/\xi$, $0 > \xi > \xi_R$, and c_2 and d_2 are constants. The integral of $\sqrt{Q(\xi)}$ cannot be evaluated in a closed form. This integral is evaluated approximately in the appropriate regimes where we need to match the JWKB solution to the solutions in the vicinity of the right-hand cutoff and the resonance.

The constants c_2, d_2, c_3, d_3 can be expressed in terms of c_1 by the procedure of uniform asymptotic matching [16]. Uniform asymptotic matching requires that:

$$\lim_{\xi \to \infty} E_{IA}(\xi) \;=\; \lim_{\xi \to \xi_R} E_{IB}(\xi) \qquad (B4a)$$

$$\lim_{\xi \to -\infty} E_{IC}(\xi) \;=\; \lim_{\xi \to 0} E_{IB}(\xi)\,. \qquad (B4b)$$

(B4a) matches the JWKB solution to the Airy function solution near the right-hand cutoff while (B4b) matches the JWKB solution to the Whittaker function solution near the resonance. The right-hand side of (B4a) can be evaluated from (B3) by approximating $Q(\xi) \approx \alpha\xi + \widetilde{\gamma} = \alpha(\xi - \xi_R)$. Then, using the asymptotic expansion for the Airy function, we get:

$$\begin{aligned} c_2 \;&=\; \frac{-i}{2\sqrt{\pi}} \alpha^{1/6} \mathrm{e}^{i\pi/4}\; c_1 \\ d_2 \;&=\; \frac{i}{2\sqrt{\pi}} \alpha^{1/6} \mathrm{e}^{-i\pi/4}\; c_1\,. \end{aligned} \qquad (B5)$$

The right-hand side of (B4b) requires that the phase-integral in (B3) be evaluated from the right-hand cutoff to a location slightly to the high-field side of the resonance. The phase-integral is evaluated by using the approximation:

$$\sqrt{Q(\xi)} \approx \sqrt{(\alpha\xi+\widetilde{\gamma})}\left[1-\frac{1}{2}\frac{\beta}{\xi(\alpha\xi+\widetilde{\gamma})}\right] . \qquad (B6)$$

In this approximation, we have assumed that in the JWKB regime $\alpha+\widetilde{\gamma}/\xi \gg \beta/\xi$ so that in (B6) we have only kept the leading order contribution due to β. Assuming $\xi_R \approx -\widetilde{\gamma}/\alpha$, we find, using (B6), that:

$$\int_{\xi_R}^{\xi} d\xi\, \sqrt{Q(\xi)} \approx \frac{2}{3\alpha}\widetilde{\gamma}^{3/2}+\sqrt{\widetilde{\gamma}}\xi-\frac{\beta}{2\sqrt{\widetilde{\gamma}}}\left\{\ln(\xi)+\ln\left(\frac{-\alpha}{4\widetilde{\gamma}}\right)\right\} . \qquad (B7)$$

Since in (B4b), $E_{IB}(\xi)$ is evaluated as $\xi \longrightarrow 0$, we approximate $[Q(\xi)]^{1/4}$ in the coefficients multiplying the phase in (B3) by $\widetilde{\gamma}^{1/4}$. Then, using the asymptotic forms of the Whittaker functions [15], we find:

$$\begin{aligned} c_3 &= \frac{1}{\widetilde{\gamma}^{1/4}}\left(\frac{\alpha}{8i\widetilde{\gamma}^{3/2}}\right)^{-i\widetilde{\eta}/2}\exp\left(\frac{2i}{3\alpha}\widetilde{\gamma}^{\frac{3}{2}}\right)c_2 \\ d_3 &= \frac{1}{\widetilde{\gamma}^{1/4}}\left(\frac{\alpha}{8i\widetilde{\gamma}^{3/2}}\right)^{i\widetilde{\eta}/2}\cdot\exp\left(-\frac{\pi\widetilde{\eta}}{2}\right)\exp\left(-\frac{2i}{3\alpha}\widetilde{\gamma}^{\frac{3}{2}}\right)d_2 \end{aligned} \qquad (B8)$$

From (B5) and (B8):

$$\frac{c_3}{d_3} = -i\left(\frac{\alpha}{8i\widetilde{\gamma}^{3/2}}\right)^{-i\widetilde{\eta}}\exp\left(\frac{\pi\widetilde{\eta}}{2}\right)\exp\left(\frac{4i}{3\alpha}\widetilde{\gamma}^{3/2}\right) . \qquad (B9)$$

It should be noted that the solution in region I is matched to the solution in region II at $\xi = 0$. From the above it is clear that:

$$\lim_{\xi\to 0^-} E_I(\xi) = \lim_{\xi\to 0^-} E_{IC}(\xi) . \qquad (B10)$$

Thus,

$$c_I = c_3 \quad \text{and} \quad d_I = d_3 . \qquad (B11)$$

REFERENCES

1. T. H. Stix, *Waves in Plasmas* (American Institute of Physics, New York, 1992).
2. A. K. Ram and A. Bers, Phys. Fluids B **3**, 1059 (1991).
3. R. Majeski, J. C. Hosea, C. K. Phillips, J. H. Rogers, G. Schilling, J. R. Wilson, S. Batha, D. Darrow, N. J. Fisch, M. C. Herrmann, D. Ignat, F. Levinton, E. Mazzucato, M. Murakami, R. Nazikian, D. Rasmussen, and E. J. Valeo, *Proceedings of the 11th Topical Conference on RF Power in Plasmas*, Palm Springs, CA, 1995, edited by R. Prater and V. S. Chan AIP COnf. Proc. 355 (American Institute of Physics, Woodbury, NY, 1995), p. 63.
4. B. Saoutic, A. Bécoulet, T. Hutter, D. Fraboulet, A. K. Ram, and A. Bers, in Ref. 3, p. 71; B. Saoutic, A. Bécoulet, T. Hutter, D. Fraboulet, A. K. Ram, and A. Bers, Phys. Rev. Lett. **76**, 1647 (1996).
5. Y. Takase, S. Golovato, M. Porkolab, R. Boivin, F. Bombarda P. Bonoli, C. Fiore, D. Garnier, J. Goetz, M. Graf, R. Granetz, M. Greenwald, S. Horne, A. Hubbard, I. Hutchinson, J. Irby, B. LaBombard, B. Lipschultz, R. Majeski, E. Marmar, M. May, A. Mazurenko, G. McCracken, P. O'Shea, R. Pinsker, J. Reardon, J. Rice, C. Rost, J. Snipes, J. Terry, R. Watterson, B. Welch, and S. Wolfe, in Ref. 3, p. 75.
6. C. Gormezano, *Proceedings of the 10th Topical Conference on RF Power in Plasmas*, Boston, MA, 1993, edited by M. Porkolab and J. Hosea, AIP Conf. Proc. 289 (American Institute of Physics, New York, 1994), p. 293.
7. A. K. Ram, A. Bers, V. Fuchs, and R. W. Harvey, in Ref. 6, p. 87.
8. T. H. Stix and D. G. Swanson, in *Handbook of Plasma Physics*, edited by M. N. Rosenbluth and R. Z. Sagdeev (North-Holland, Amsterdam, 1983), Chapter 2.4.
9. K. G. Budden, *The Propagation of Radio Waves* (Cambridge University Press, Cambridge, 1985), pp. 596-602.
10. J. Jacquinot, B. D. McVey, and J. E. Scharer, Phys. Rev. Lett. **39**, 88 (1977).
11. R. Majeski, C. K. Phillips, and J. R. Wilson, Phys. Rev. Lett. **73**, 2204 (1994).
12. A. K. Ram, A. Bers, V. Fuchs, and S. D. Schultz, in *Controlled Fusion and Plasma*

Physics, Proceedings of the 21st EPS Conference (European Physical Society, Geneva,1994), Vol. 18B, Part III, p. 1134; A. K. Ram, A. Bers, V. Fuchs, and S. D. Schultz, in *Proceedings of the 15th International Conference on Plasma Physics and Controlled Nuclear Fusion Research* (International Atomic Energy Agency, Vienna, 1994), Paper No. IAEA-CN-60/D-P-I-15; V. Fuchs, A. K. Ram, S. D. Schultz, A. Bers, and C. N. Lashmore-Davies, Phys. Plasmas **2**, 1637 (1995).

13. M. Abramowitz and I. A. Stegun, *Handbook of Mathematical Fuctions*, (Dover, New York, 1970).
14. H. Buchholz, *The Confluent Hypergeometric Function* (Springer-Verlag, New York, 1969).
15. J. Heading, J. Math. Soc. London **37**, 195 (1962).
16. C. M. Bender and S. A. Orszag, *Advanced Mathematical Methods for Scientists and Engineers* (McGraw-Hill, New York, 1978).

Figure Captions

FIG. 1 The real part of $k_\perp^2$, obtained from the local hot-plasma dispersion relation, as a function of distance along the equatorial plane for TFTR-type parameters [3]. The plasma consists of D, ^{3}He, ^{4}He, and C ions. The ratios of the ion densities to the electron density are 0.12, 0.25, 0.1, and 0.03, respectively. The major radius is 2.62 m, the plasma radius is 0.95 m, the peak electron density $n_0 = 5.5 \times 10^{19}$ m^{-3}, the central toroidal magnetic field is 4.8 Teslas, the frequency of the FAW is 43 MHz, the peak electron and ion temperatures are 6.5 keV, the density profile is parabolic and the temperature profile is parabolic-squared. Here $k_\parallel$ (the component of the wavevector along the magnetic field) is assumed to be 6 m^{-1}. Also $x_{\rm RES}$, $x_{\rm LHC}$, $x_{\rm HFS-RHC}$, and, $x_{\rm LFS-RHC}$ are the locations of the ion-ion hybrid resonance, the left-hand cutoff, the high-field side right-hand cutoff, and the low-field side right-hand cutoff, respectively.

FIG. 2 A magnified view of the mode-conversion region showing the coupling between FAW and IBW.

FIG. 3 Contours of constant mode-conversion coefficient as a function of η and ϕ.

FIG. 4 Contours of maximum mode-conversion as function of peak electron density and $k_\parallel$. The parameters are the same as for Fig. 1.

FIG. 5 The model potential of Eq. (8) for $\alpha = 351$, $\beta = 5$, and $\gamma = \widetilde{\gamma} = 513.6$. The locations of the high-field side right-hand cutoff, the ion-ion hybrid resonance, and the left-hand cutoff are denoted by $\xi_{\rm HFS-RHC}$, $\xi_{\rm RES}$, and $\xi_{\rm LHC}$, respectively.

FIG. 6 The field solution, $|E|$, to Eq. (2) for the $Q(\xi)$ given in Fig. 5. The parameters chosen were such that the reflection coefficient is almost zero and the entire incoming FAW power is mode converted.

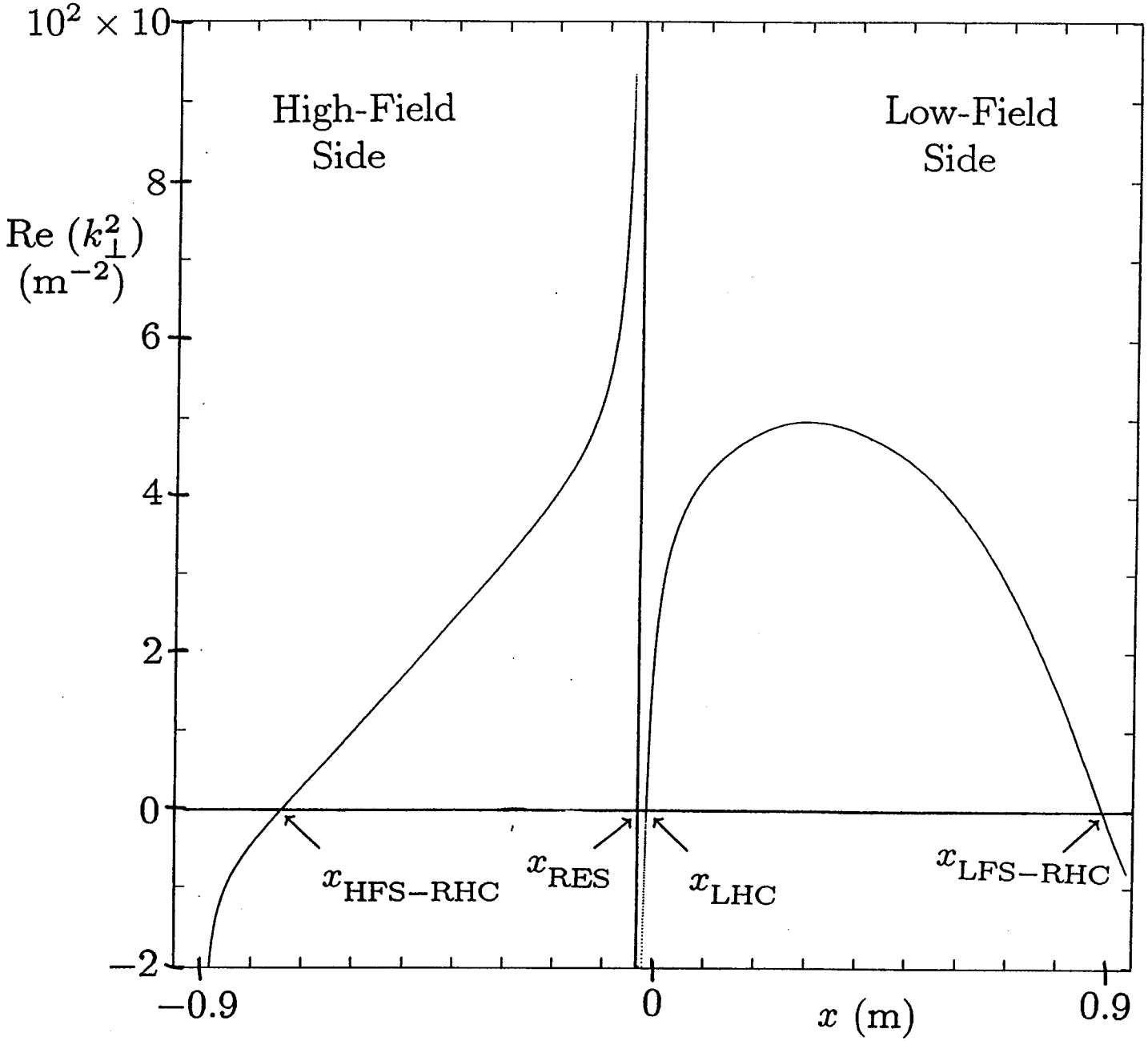

Fig. 1 A. K. Ram et. al. Phys. Plas.

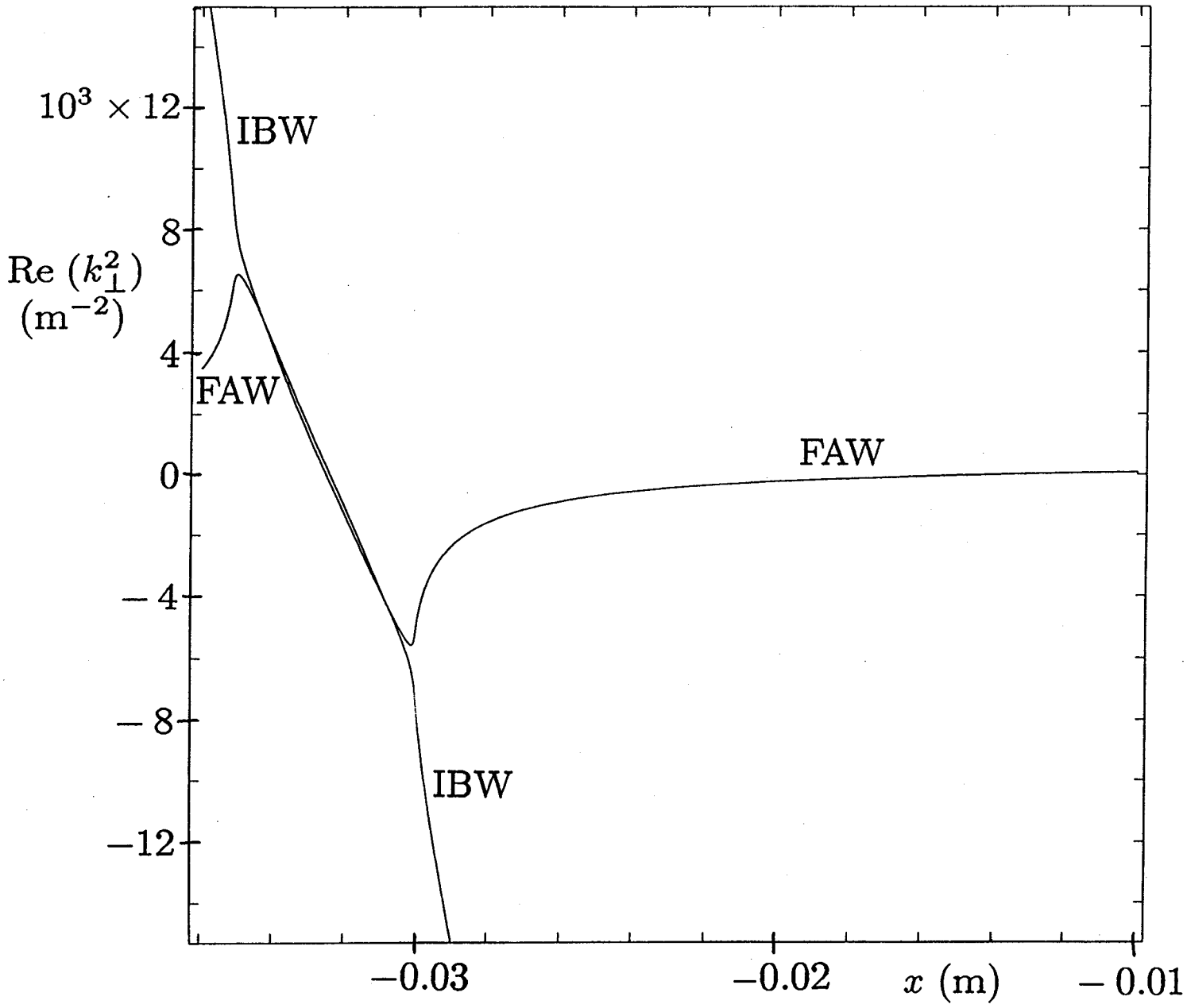

Fig. 2 A. K. Ram et. al. Phys. Plas.

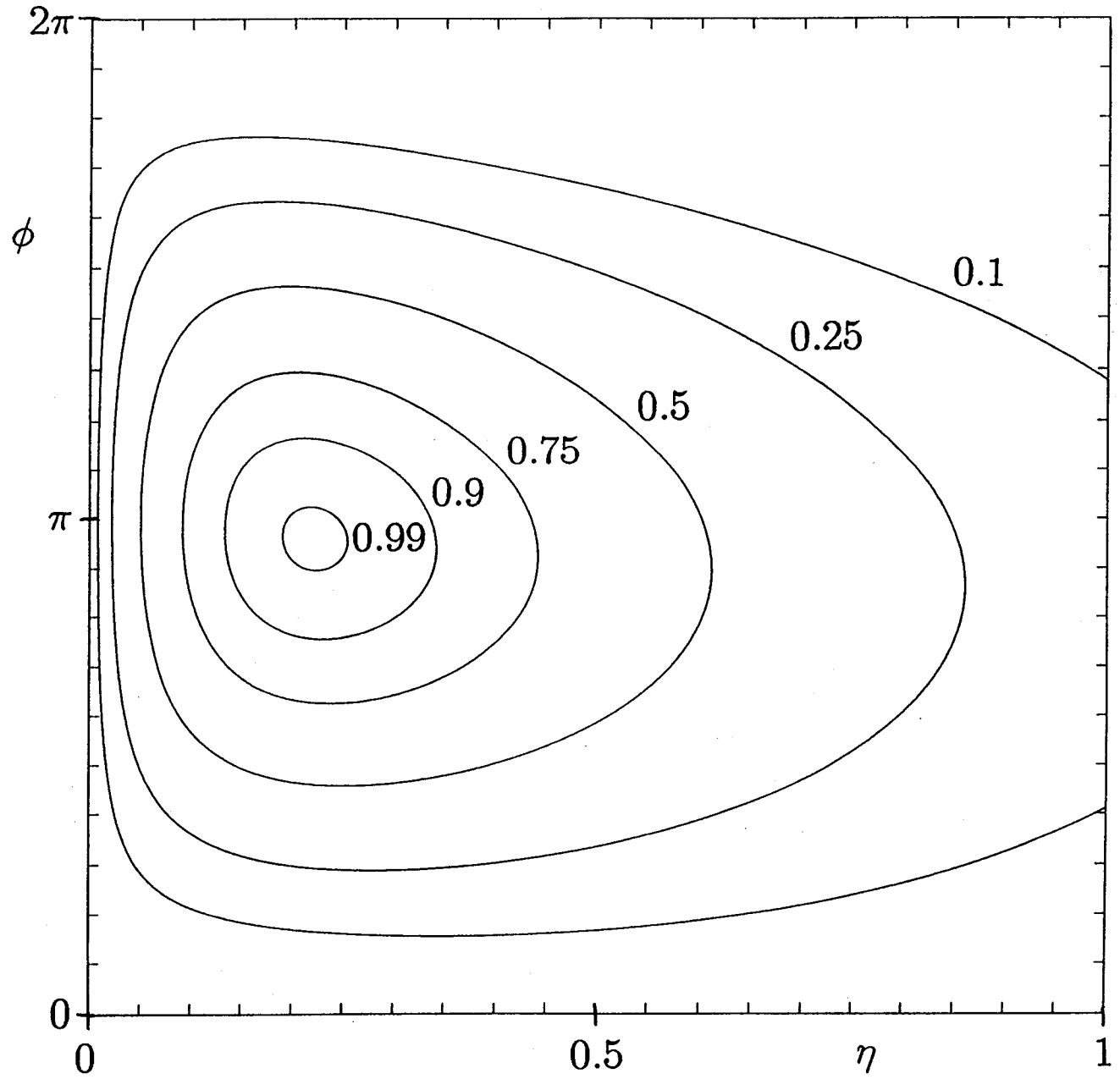

Fig. 3 A. K. Ram et. al. Phys. Plas.

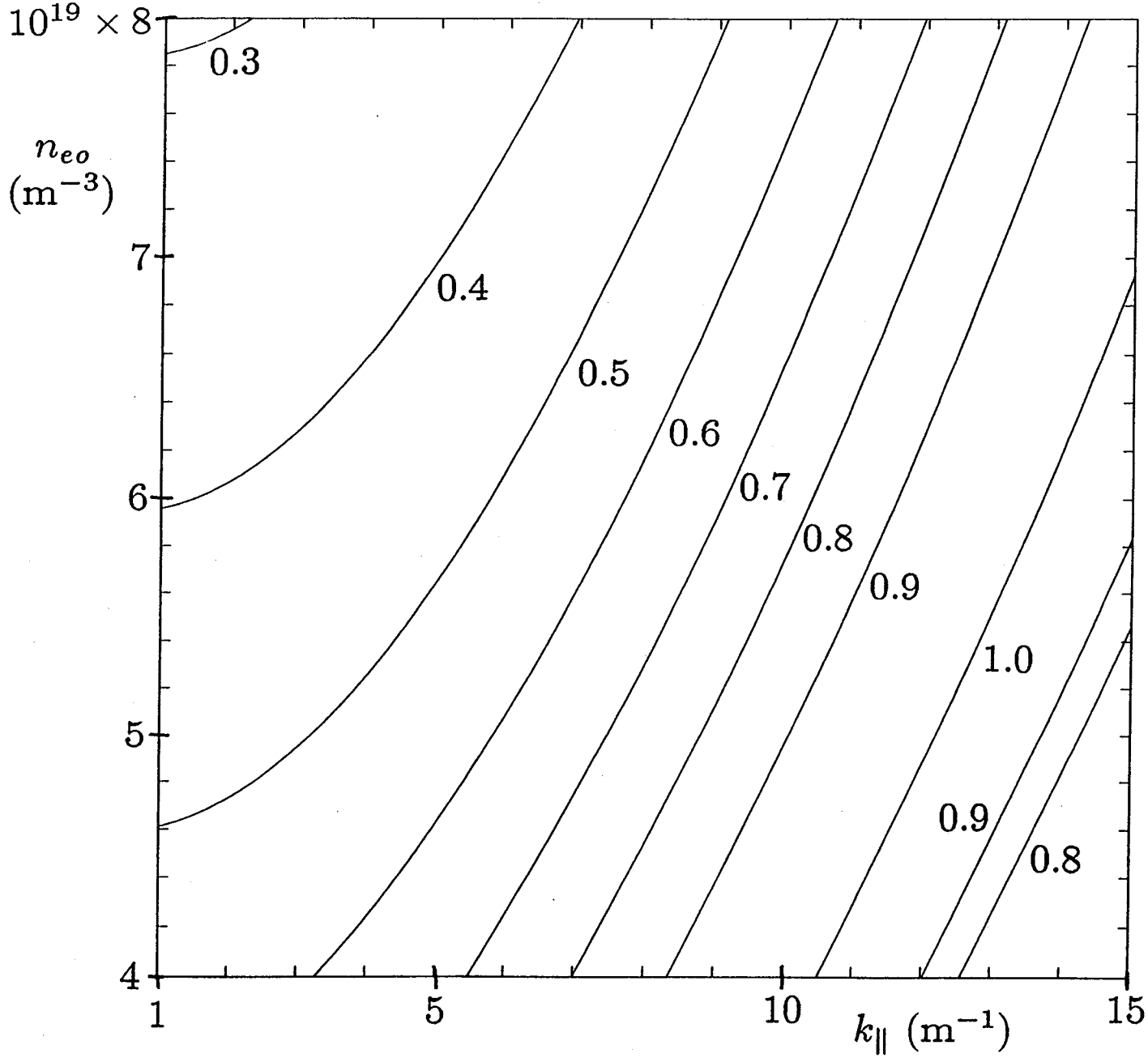

Fig. 4 A. K. Ram et. al. Phys. Plas.

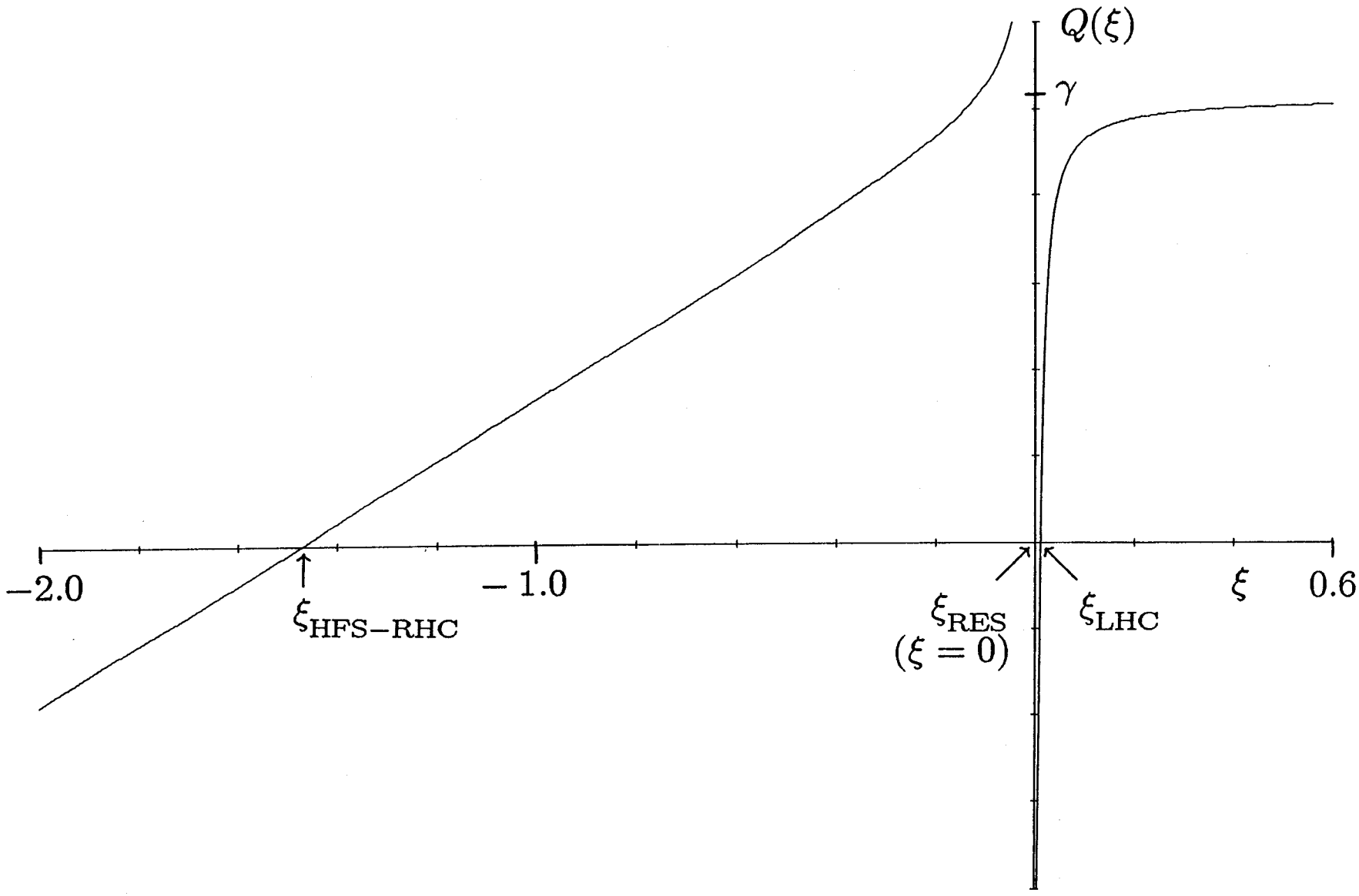

Fig. 5 A. K. Ram et. al. Phys. Plas.

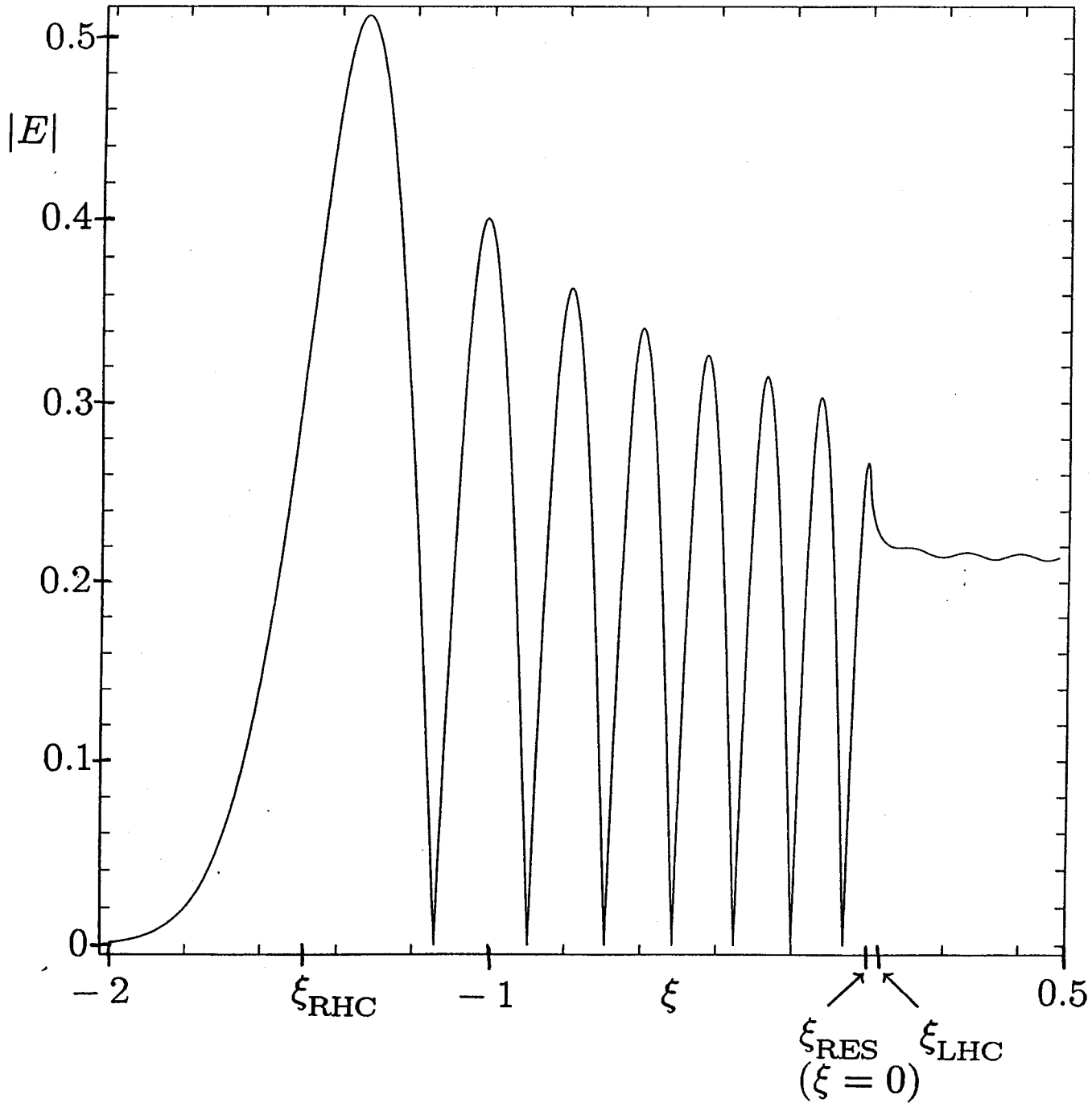

Fig. 6 A. K. Ram et. al. Phys. Plas.